METHOD OF CALCULATION OF HEAT-TRANSFER COEFFICIENTS FOR THE X-15 AIRPLANE

By William V. Feller

Langley Aeronautical Laboratory

One of the principal missions of the X-15 airplane is to investigate the high aerodynamic heating rates which are expected in hypersonic flight. However, in order to design the airplane to perform this mission safely and effectively, the designer must have some idea of the magnitude of the heating rates to which the airplane will be exposed.

One of the major unknowns in the design of the airplane is how much of the boundary layer will be laminar. Available theoretical and experimental studies indicate the possibility of extensive areas of laminar flow at the conditions under which the airplane will fly. However, the surface of the airplane probably will not be as fair and polished as those on laboratory models, so the prediction of the extent of laminar flow on the basis of model tests cannot be relied on. Conservative design would require that nearly all of the airplane be assumed to have a turbulent boundary layer. If, in flight, the airplane is found to have long runs of laminar boundary layer, it will be desirable to trip transition artificially in some flights in order to study turbulent heating rates.

The flow field around the complete airplane configuration is far too complex to permit calculation of the heat transfer including interference or interaction between the parts of the airplane. Therefore, it is necessary to consider isolated parts of the airplane, and in some cases approximate those by bodies of simpler shapes for which theoretical or experimental studies are available.

Figure 1 shows a breakdown of the airplane into the parts which will be discussed in this paper. The wing (and tail surfaces) can be divided into two elements: the swept cylinder leading edge, and the rest of the wing, which is so slightly curved that it can be considered a flat plate. In the combination, however, there is the additional consideration of how the shock wave from the cylinder affects the heat transfer over the plate portion. The dive brakes will be treated as flat plates at angle of attack. The fuselage nose is actually a part of a sphere. The fuselage, omitting the side tunnels and canopy, is a body of revolution. Calculations can be made for this shape at zero angle of attack in laminar flow, and in turbulent flow it can be approximated by considering the surface locally a flat plate but using the varying local flow conditions. At small angles of attack, the flow pattern over the body can be considered similar to that at zero angle and the same procedures can be applied, with modifications of the local flow conditions because of the angle of attack. At

high angles of attack, however, the flow around the fuselage will more nearly resemble that on a swept cylinder.

Consider first the wing, which is thin (about 0.05 chord) and has a semicircular-section leading edge with a 3/4-inch diameter. Except for the regions influenced by the tip and by the fuselage (neglecting for the moment the effect of the bow shock from the fuselage nose) the wing can be approximated by a flat plate with a swept-circular-cylinder leading edge.

The X-15 project has stimulated work on swept cylinders, both theoretical and experimental (refs. 1 to 5), so that the heat transfer to the cylindrical part of the leading edge can be calculated with confidence. At some distance back from the leading edge the heat transfer should be nearly that for a flat plate which has also been extensively studied (refs. 6 to 8). The question is how the two calculations should be joined.

Figure 2 shows some wind-tunnel test results which, while not for the same configuration as the X-15 wing, give some idea of the trend to be expected. The model tested was a slab wing with a semicircular leading edge swept 60°. Tests were made in the Langley 11-inch hypersonic tunnel at zero angle of attack, $M = 6.86$, and a Reynolds number of 0.214×10^6 based on cylinder diameter and free-stream conditions. The ordinate in figure 2 (on a logarithmic scale) is the dimensionless heat-transfer parameter $N_{St}\sqrt{R_D}$ which is used to correlate laminar heat-transfer results at different Reynolds numbers, and the abscissa is X/D, the distance from the stagnation point (measured in the streamwise direction) divided by the leading-edge diameter.

Over the cylinder the experimental values of the heat-transfer parameter $N_{St}\sqrt{R_D}$ agree well with the theory of Goodwin, Creager, and Winkler for swept cylinders (ref. 1). This kind of agreement has been found at several Mach numbers and over a wide range of Reynolds numbers, so that the theory can be considered well established.

For the flat-plate portion of the wing, two curves are shown for both laminar and turbulent flow, which were calculated from the laminar and turbulent theories of Van Driest (refs. 6 and 7). The upper curve in each case (dashed) is for a flat plate at the free-stream conditions, neglecting the effect of the shock from the blunt leading edge. This can be expected to be valid a long distance downstream, where the effect of the strong shock due to the cylinder has been dissipated. The lower curve for each type of boundary layer is calculated by using the total pressure behind the bow shock and then expanding to free-stream pressure to determine the conditions for the flat-plate calculation of heat transfer. The validity of this procedure has been verified experimentally in reference 9 and elsewhere for distances of several nose diameters along the flat plate.

At 60° sweep as in these tests, the heat-transfer coefficients calculated with and without the leading-edge shock are not very different. This is due to a compensating effect - although the local Mach number is lower over the surface affected by the leading-edge shock, the local temperatures are higher and the net result is to bring the curves for the heat-transfer coefficients nearly together. The experimental-data points in figure 2 indicate that the heat-transfer coefficients fall from the value on the cylinder fairly quickly, and in about two leading-edge diameters are close to the values calculated for the flat plate. The data then rise, indicating transition, and approach the turbulent curves.

These data give no indication of how far back on the plate the effect of the shock from the cylinder might be felt. There has been some study of the effect of a blunt leading edge on the pressures over a plate (ref. 10) which indicates that the pressure is still 10 percent higher than free-stream pressure at a distance of 70 leading-edge diameters downstream.

For a given wing profile, a more accurate approach would be to calculate the local pressures over the profile and use these to determine the local flow properties, which are then inserted into the flat-plate theory to determine the local heat-transfer coefficients. There are also more exact theories which can be applied for a given profile if the local velocity outside the boundary layer can be approximated by a power-law variation with distance from the stagnation point. For very thin wings, however, the simpler flat-plate calculation can be expected to give good engineering accuracy in the heat-transfer calculations.

Figure 3 shows a sample of the application of the simple cylinder and flat-plate theories to the X-15 airplane wing at an angle of attack. The conditions assumed are $M = 6.0$, an altitude of 102,000 feet, and an angle of attack of 26°, for which the local Reynolds numbers near the nose are small enough to assure laminar flow.

Values of the heat-transfer coefficient on the nose were calculated from the laminar swept-cylinder theory for an effective sweep angle of 32.75°, which includes the effect of angle of attack in reducing the sweep angle. Two curves are shown for the lower surface behind the cylinder. The dashed line is the heat-transfer coefficient calculated by using the flow conditions behind the shock wave appropriate to a sharp-edge plate at an angle of attack of 26°. The solid line was calculated by using the total pressure at the stagnation point of the cylinder with 32.75° sweep and expanding isentropically to the pressure determined by the plane shock for an angle of attack of 26°, the same pressure as was used for the sharp-edge-plate calculation. For design purposes, transition was arbitrarily assumed to occur 4 inches from the leading edge, and for both laminar and turbulent flow in each of the calculations the flat-plate leading edge was assumed to coincide with the actual wing leading edge.

Near the leading edge, the effect of bluntness should be predominant, and the heat-transfer values should be close to the solid curve in the laminar regions and some distance back in the turbulent regions. However, farther back on the wing the flow affected by the small region of the curved shock at the leading edge must eventually become submerged in the boundary layer, after which the heat-transfer coefficients will approach the dashed line, their values being determined by the conditions behind the plane shock.

The difference between the two calculations in the turbulent region is appreciable. However, it is not yet clear how far back the effect of bluntness can be expected to continue, particularly at an angle of attack.

On the upper surface, behind the nose, the heat-transfer coefficients are computed with the assumption that the flow separates from the leading edge of the flat plate. In the method used, which is based on results from a limited number of wind-tunnel tests, the separated-flow heat-transfer coefficients were assumed to be half those for a flat plate at zero angle of attack. The whole problem of heat transfer in separated flows has been studied very little and considerable work must be done to establish the actual behavior, but for design purposes the significant fact is that the heat-transfer coefficients are very low compared with those on the lower surface. The rough estimate based on 1/2 the value for a flat plate at zero angle of attack is a conservative one. If the flow should remain attached, the heat-transfer coefficients would be lower still.

The effect of the fuselage bow shock on the wing will require study with the complete model. The actual line of intersection of the shock and the wing will move around as the shock-wave angle changes with the changing Mach number and angle of attack in a flight, and thus local effects at the shock-surface intersections will be spread out. The conditions used in calculating the heat transfer on the rest of the wing behind the shock must include the effect of the fuselage shock.

Another area of high heat transfer is on the dive brakes when they are extended. The specific X-15 configuration has not been tested, but an insight into the method of calculating the heat transfer to the dive brakes can be obtained from the results shown in figure 4, which were obtained on a flare at the rear of a body of revolution at $M = 6.86$. This figure has been taken from reference 11. The heat-transfer data on the forward part of the body follow the laminar curve, but the coefficients rise on the cylinder and indicate that just ahead of the flare the boundary layer is turbulent. In this case the shock was attached at the cylinder-flare juncture. Because the static-pressure rise across the shock is large, the body boundary layer has only a small effect on the flare boundary layer. Therefore, except very near the juncture, the heat transfer can be calculated as though the boundary layer starts at

zero thickness at the juncture. The theoretical curve shown in figure 4 was calculated by using the turbulent flat-plate theory of Van Driest (ref. 7) and the local flow conditions behind the shock wave. It can be seen in this figure that the experimental measurements are in good agreement with values calculated for a flat plate at the conditions behind the shock. A similar approach would appear to be reasonable on the dive brakes of the X-15.

The nose of the fuselage consists of a 6-inch-diameter sphere mounted in a socket which permits rotation. The sphere is instrumented to measure angles of attack and yaw, as described in a subsequent paper by I. Taback and G. M. Truszynski. In flight, the Reynolds number on the sphere will be low enough to permit the assumption of laminar boundary layer.

Figure 5 shows the distribution of the dimensionless heat-transfer parameter $N_{St}\sqrt{R_D}$ around the sphere and on the lower side of the mounting structure at $M = 6.86$. On the sphere, experimental values agree well with the laminar theory of Stine and Wanlass for bodies of revolution. (See ref. 12.) On the stagnation point of the lower lid, however, the heat-transfer rates are very large. Schlieren photographs of this configuration show a shock in the flow just ahead of this point. The problem is being studied further to determine how to reshape the support cone to reduce the heating rates to tolerable values. The heat-transfer values on the upper side of the support cone are very low - too small to show at this scale.

The fuselage of the X-15 is basically a body of revolution with side fairings attached. This is an awkward shape for theoretical calculations. For zero angle of attack, it may be possible to neglect the distortion of the cross section and treat the body, or at least the part of it outside the fairings, as a body of revolution, for which theory and experimental verification are available.

Figure 6 shows preliminary results for a body of revolution similar to the X-15 nose at conditions giving laminar flow. The body was a Karman nose with a fineness ratio of 5, modified by the addition of a tangent 10° half-angle cone in front and followed by a short section of cylinder. This shape is not the X-15 nose shape, but the distribution of heat transfer should be similar.

The circles are $N_{St}\sqrt{R_D}$ plotted on a logarithmic scale from tests at $M = 6.86$ with laminar boundary layer. On the conical tip, the data agree well with the cone theory obtained by applying the Mangler transformation for cones to the flat-plate theory. The experimental data fall off from the cone values as the body shape varies from conical and reach good agreement with the laminar flat-plate theory on the cylinder. The laminar theory of Stine and Wanlass (ref. 12) for this body of revolution

at $M = 6.86$ is shown merging into the curve for the cone at the forward end and meeting the flat-plate calculation at the cylinder, and it is in good agreement with the data over the entire nose.

The squares are values obtained on the same body at $M = 3.69$ in the Langley Unitary Plan wind tunnel at a higher Reynolds number. The values are very close to those for $M = 6.86$, as is the Stine and Wanlass theory for $M = 3.69$, indicating that for laminar boundary layers the Mach number effect over this range is small.

Another series of tests was made on the same model at $M = 3.69$ with roughness applied in a ring near the nose to give a turbulent boundary layer. The preliminary experimental results are shown in figure 7 by circles. Also shown is the turbulent theory for the cone at the nose, calculated by the method of reference 13, and for the flat plate with the use of local flow conditions on the cylinder. The data show roughly the same pattern as was shown for laminar flow, a trend from values near those of the cone at the forward end down to the flat-plate values on the cylinder. There is as yet no turbulent analog of the Stine and Wanlass theory, but experimental data like these can be used to fit an empirical curve for the transition between the cone and flat-plate calculations.

At angles of attack, the prediction of heat transfer to bodies becomes much more uncertain. There is no generally applicable theory such as the Stine and Wanlass theory for zero angle of attack in laminar flow. At small angles of attack, the streamlines around the body should be nearly longitudinal, and an approximation can be made by using cone or flat-plate theory with varying local conditions along the length. At large angles of attack, the body can be approximated by a swept cylinder with varying diameter.

These two kinds of approximation are shown in figure 8 for a turbulent boundary layer. The variation of the nondimensional heat-transfer parameter N_{St} with angle of attack is shown for the lower or windward stagnation line at two stations along the length of the same modified Karman nose discussed earlier at $\alpha = 0$. The curves labeled "longitudinal flow theory" were calculated by using the flat-plate heat-transfer relations for turbulent flow with the local conditions at the two stations.

Local conditions were calculated for each angle of attack by finding the pressure on a cone at zero angle of attack tangent to the lower stagnation line at the nose, and then expanding two-dimensionally along the body to the local body inclination.

The curves labeled "crossflow theory" were computed by assuming that at each station the shock was that appropriate for the tangent cone of the local inclination angle, and then calculating the stagnation-line turbulent heat transfer from the swept-cylinder theory of reference 5, using conditions behind the cone shock.

The experimental points are from tests in the Langley Unitary Plan wind tunnel, with roughness applied in a strip along the lower stagnation line and in a ring at the nose. It can be seen that the data agree fairly well with the crossflow theory at the higher angles and with the longitudinal-flow theory at zero angle of attack, but the experimental points suggest a more rapid increase with angle of attack than is predicted by the longitudinal-flow calculation at small angles and a change in the trend between 14° and 21°. There is need for further work to develop an approach that will be more nearly adequate for moderate angles than either of those described here.

The use of crossflow theory at high angles of attack is further corroborated in figure 9, which shows in polar coordinates the distribution of heat-transfer coefficients around the body at the $X/D = 5.1$ station, where the body is cylindrical. Data are presented for angles of attack of 0°, 7°, 14°, 21°, and 25°. The theoretical curve for $\alpha = 25^\circ$ was obtained by using the theoretical correlation parameter presented in reference 5 with some unpublished experimental results by the same authors for the distribution of local heat-transfer rates around a swept cylinder with turbulent flow from the stagnation line. At 25° the agreement of theory and experimental values is good.

The data for $\alpha = 14^\circ$ and $\alpha = 21^\circ$ fall very nearly on the same curve. This result indicates the need, mentioned before, for further study in this range.

The wind-tunnel results presented in this paper have been compared with available theories to give some indication of how well the theories can be expected to predict the heat transfer to the full-scale airplane. In general, for isolated parts of the airplane which can be approximated by simple shapes, the heat transfer can be satisfactorily predicted by available theories. For regions where there is interference between the flows on adjacent parts - for example, the wing-fuselage juncture, cockpit canopy, and side fairings - more detailed studies are required on the specific configuration, and for this purpose a complete scale model is being prepared by North American Aviation for wind-tunnel tests in the Langley Unitary Plan wind tunnel.

REFERENCES

1. Goodwin, Glen, Creager, Marcus O., and Winkler, Ernest L.: Investigation of Local Heat-Transfer and Pressure Drag Characteristics of a Yawed Circular Cylinder at Supersonic Speeds. NACA RM A55H31, 1956.

2. Eggers, A. J., Jr., Hansen, C. Frederick, and Cunningham, Bernard E.: Theoretical and Experimental Investigation of the Effect of Yaw on Heat Transfer to Circular Cylinders in Hypersonic Flow. NACA RM A55E02, 1955.

3. Beckwith, Ivan E.: Theoretical Investigation of Laminar Heat Transfer on Yawed Infinite Cylinders in Supersonic Flow and a Comparison With Experimental Data. NACA RM L55F09, 1955.

4. Feller, William V.: Investigation of Equilibrium Temperatures and Average Laminar Heat-Transfer Coefficients for the Front Half of Swept Circular Cylinders at a Mach Number of 6.9. NACA RM L55F08a, 1955.

5. Beckwith, Ivan E., and Gallagher, James J.: Experimental Investigation of the Effect of Boundary-Layer Transition on the Average Heat Transfer to a Yawed Cylinder in Supersonic Flow. NACA RM L56E09, 1956.

6. Van Driest, E. R.: Investigation of Laminar Boundary Layer in Compressible Fluids Using the Crocco Method. NACA TN 2597, 1952.

7. Van Driest, E. R.: Turbulent Boundary Layer in Compressible Fluids. Jour. Aero. Sci., vol. 18, no. 3, Mar. 1951, pp. 145-160, 216.

8. Rubesin, M. W., and Johnson, H. A.: A Critical Review of Skin-Friction and Heat-Transfer Solutions of the Laminar Boundary Layer of a Flat Plate. Trans. A.S.M.E., vol. 71, no. 4, May 1949.

9. Crawford, Davis H., and McCauley, William D.: Investigation of the Laminar Aerodynamic Heat-Transfer Characteristics of a Hemisphere-Cylinder in the Langley 11-Inch Hypersonic Tunnel at a Mach Number of 6.8. NACA TN 3706, 1956.

10. Bertram, Mitchel H.: Viscous and Leading-Edge Thickness Effects on the Pressures on the Surface of a Flat Plate in Hypersonic Flow. Jour. Aero. Sci. (Readers' Forum), vol. 21, no. 6, June 1954, pp. 430-431.

11. Becker, John V., and Korycinski, Peter F.: Heat Transfer and Pressure Distribution at a Mach Number of 6.8 on Bodies With Conical Flares and Extensive Flow Separation. NACA RM L56F22, 1956.

12. Stine, Howard A., and Wanlass, Kent: Theoretical and Experimental Investigation of Aerodynamic-Heating and Isothermal Heat-Transfer Parameters on a Hemispherical Nose With Laminar Boundary Layer at Supersonic Mach Numbers. NACA TN 3344, 1954.

13. Van Driest, E. R.: Turbulent Boundary Layer on a Cone in a Supersonic Flow at Zero Angle of Attack. Jour. Aero. Sci., vol. 19, no. 1, Jan. 1952, pp. 55-57, 72.

BREAKDOWN OF AIRPLANE FOR HEAT-TRANSFER CALCULATIONS

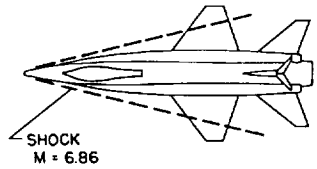

WING AND TAIL SURFACES
- LEADING EDGE
- FLAT PLATE (WITH AND WITHOUT BOW SHOCK)
- EFFECTS OF FUSELAGE SHOCK

DIVE BRAKE, EXTENDED

FUSELAGE NOSE

FUSELAGE
- ZERO ANGLE OF ATTACK
- LOWER STAGNATION LINE AT ANGLE OF ATTACK
  - LONGITUDINAL FLOW
  - CROSS FLOW

Figure 1

HEAT TRANSFER TO 60° SWEPT WING

$\alpha = 0°$; $M = 6.86$; $R_D = 0.214 \times 10^6$

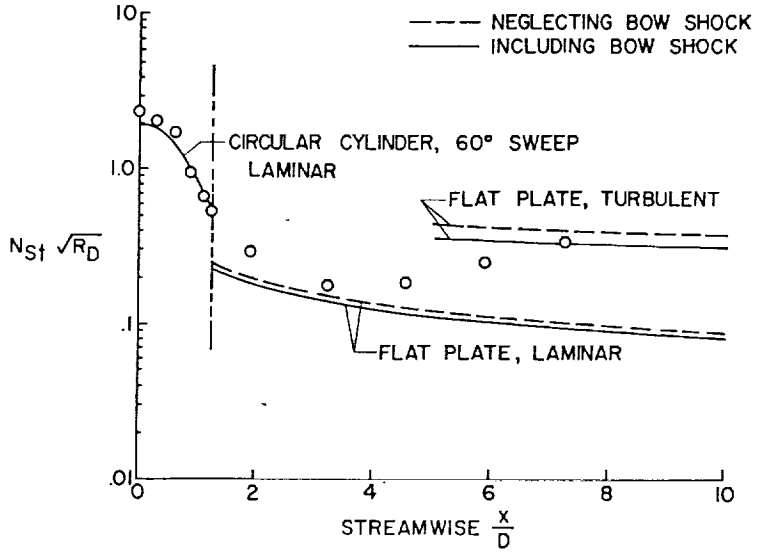

Figure 2

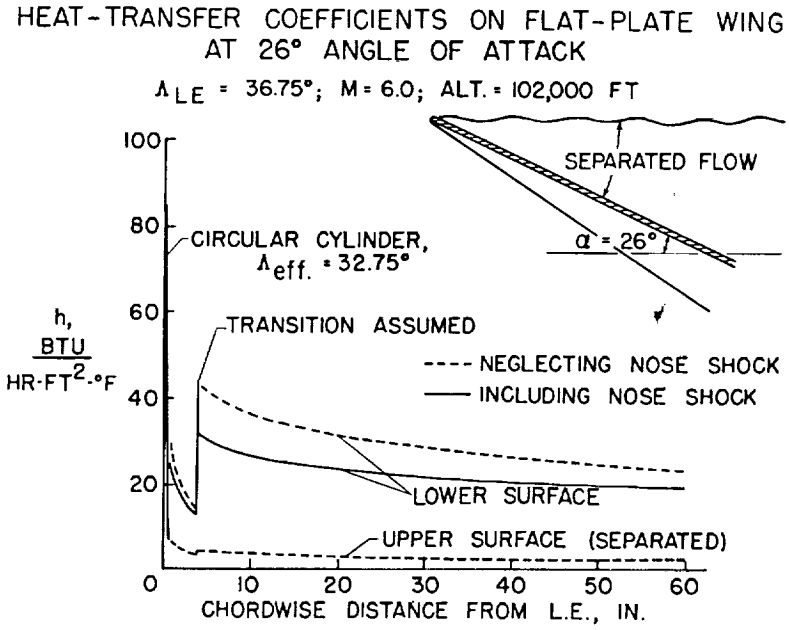

Figure 3

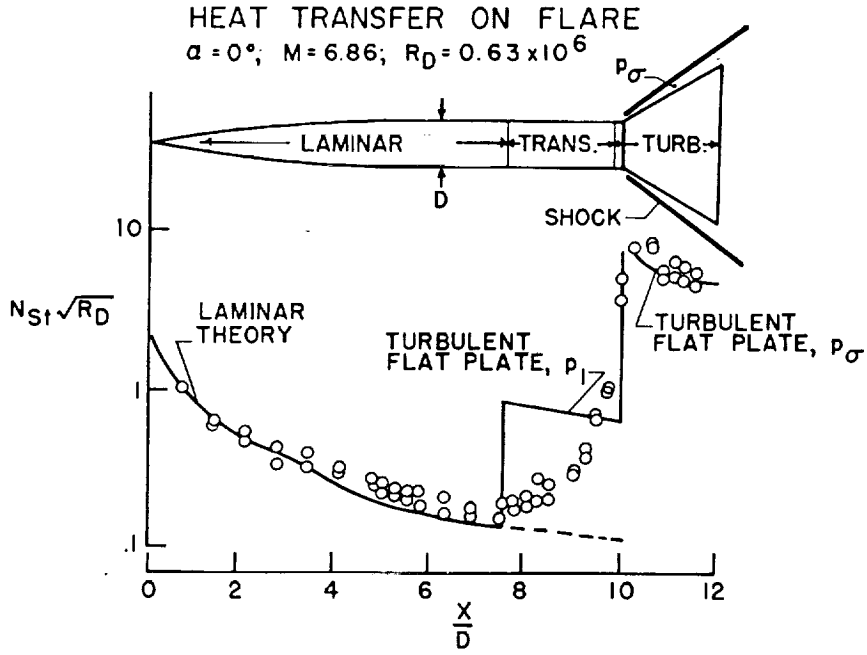

Figure 4

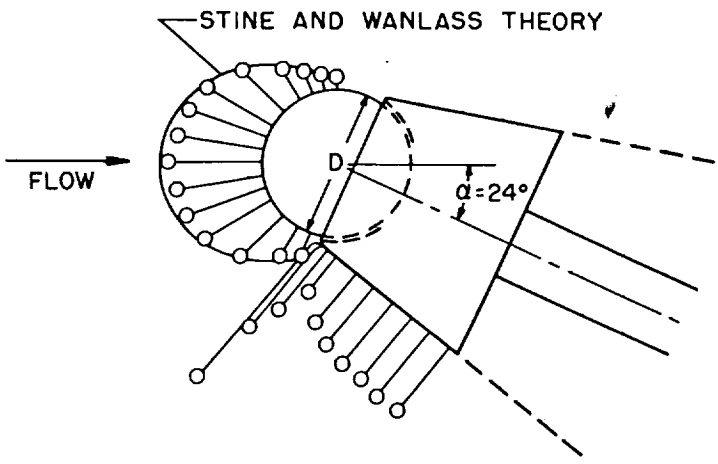

Figure 5

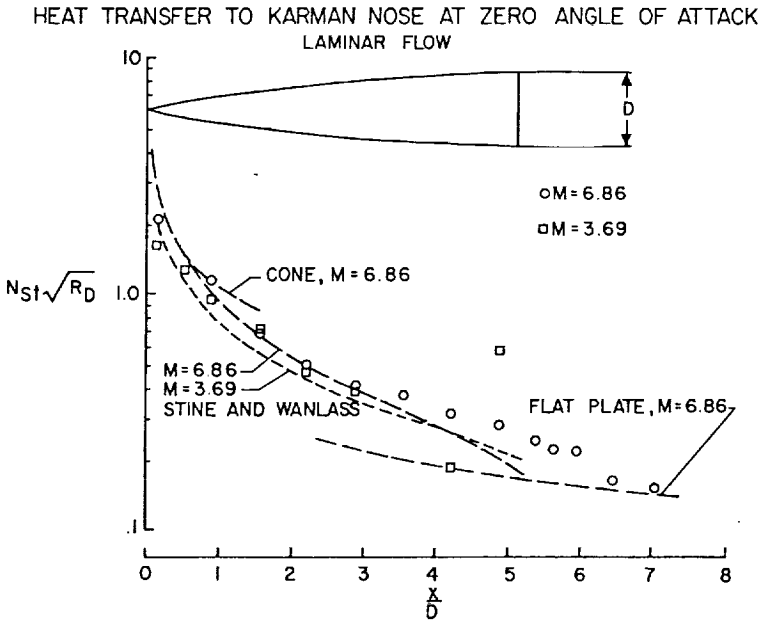

Figure 6

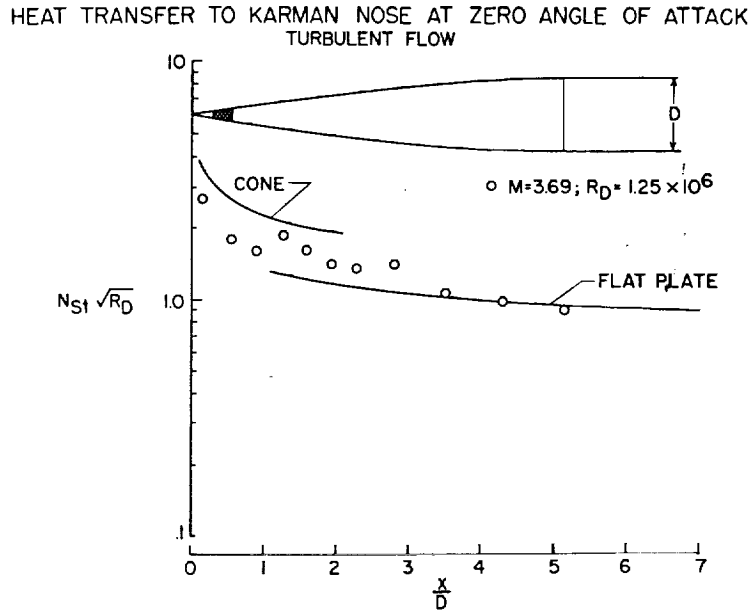

Figure 7

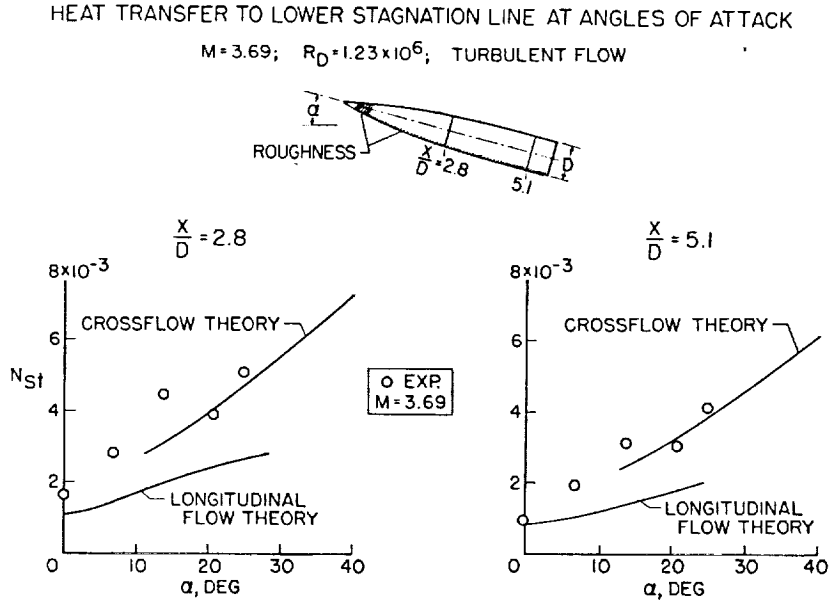

Figure 8

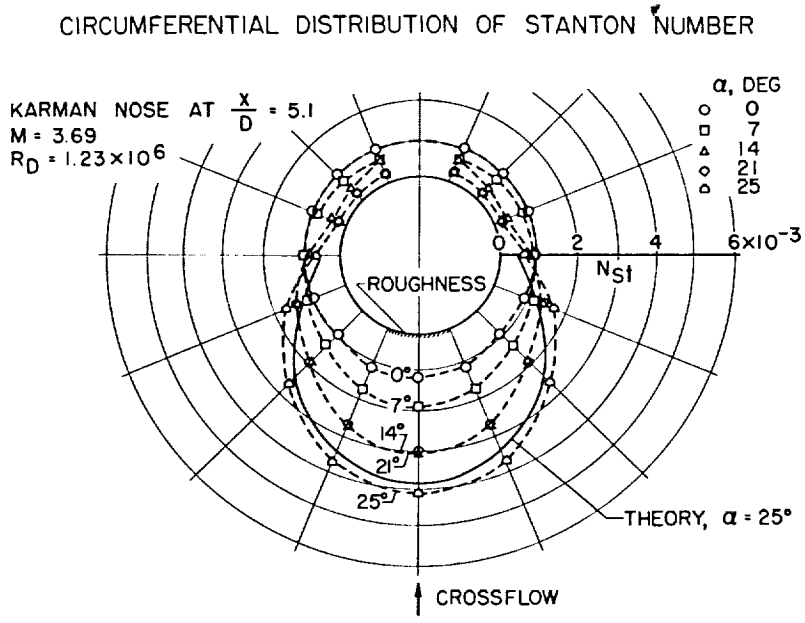
CIRCUMFERENTIAL DISTRIBUTION OF STANTON NUMBER
KARMAN NOSE AT X/D = 5.1
M = 3.69
R_D = 1.23×10^6
α, DEG
0
7
14
21
25
0
2
4
6×10^-3
N_St
ROUGHNESS
0°
7°
14°
21°
25°
THEORY, α = 25°
CROSSFLOW

Figure 9